

1-2-1990

## Azimuthal Variations of Sensitivity in the Coaxial Scanning Auger Microprobe

L. Frank

*Czechoslovak Academy of Sciences*

Follow this and additional works at: <https://digitalcommons.usu.edu/microscopy>



Part of the [Biology Commons](#)

---

### Recommended Citation

Frank, L. (1990) "Azimuthal Variations of Sensitivity in the Coaxial Scanning Auger Microprobe," *Scanning Microscopy*: Vol. 4 : No. 1 , Article 8.

Available at: <https://digitalcommons.usu.edu/microscopy/vol4/iss1/8>

This Article is brought to you for free and open access by the Western Dairy Center at DigitalCommons@USU. It has been accepted for inclusion in Scanning Microscopy by an authorized administrator of DigitalCommons@USU. For more information, please contact [digitalcommons@usu.edu](mailto:digitalcommons@usu.edu).



## AZIMUTHAL VARIATIONS OF SENSITIVITY IN THE COAXIAL SCANNING AUGER MICROPROBE

L. Frank

Institute of Scientific Instruments, Czechoslovak Academy of Sciences,  
Brno, Czechoslovakia

(Received for publication August 29, 1989, and in revised form January 2, 1990)

### Abstract

Experiments with the PHI 595 Multiprobe have revealed a pronounced asymmetry of the energy filtered image (the shape of the line-scan curve) obtained with an isolated sphere lying on a flat surface. The effect is explained as a consequence of transmission efficiency variations along the circumference of the ring-shaped detector assembly, and is probably caused by deviations from coaxiality of the adjustable parts of the entrance annular aperture controlling the energy resolution. A quantitative model provides realistic results and has indicated the emission anisotropy of Auger electrons as being much larger than that of the energy filtered background emission at various energies.

### Introduction

The main advantage claimed for the coaxial scanning Auger microprobe, in particular, the Perkin Elmer Multiprobe series, is the symmetrical configuration of the detector system that provides high collection efficiency and reduces shadowing and topographic effects with rough samples. Inherent in the coaxial microscope/analyzer geometry is the necessity to capture the energy filtered electrons in an off-axis detector since the optical axis is occupied by the primary beam (see Fig.1). The cylindrical mirror analyzer (CMA) is therefore used in the annular aperture mode (Risley, 1972) which is much more tolerant of stray magnetic fields of the microscope (Gerlach, 1980). On the other hand, it is taken for granted that the detector actually has constant sensitivity around the whole circumference. If this were not the case, the outstanding properties mentioned above would be weakened and certain shadowing contrast would appear in the elemental mappings of rough surfaces.

In front of the detector is placed an annular aperture consisting of two mutually adjustable parts. It is used for controlling the energy resolution of the CMA. No facilities are provided for centering the aperture, which is precentered by the manufacturer.

### Experimental

To test the axial symmetry of the PHI 595 Multiprobe sensitivity, it is suitable to make use of analytical imaging of well defined surfaces, preferably a spherical surface, allowing straightforward determination of angles of incidence and of emission. In our case, small Cr spheres were used, attached with carbon paste onto a Si surface (see Fig.2). The spheres were extracted from a metal powder used in hard vacuum soldering.

For the above-mentioned study it was necessary to avoid other possible asymmetries in the experimental configuration. This means that one should use the as-supplied spherical surface only, since the oblique impact of Ar ions used in the instrument for surface cleaning would cause inhomogeneous changes in both the topography and the chemical composition. The 30° sample holder falls well within the range of polar angles enabling a symmetrical image signal to be obtained from the sphere (Gerlach, 1985) (as no shadowing of the analyzer entrance by the holder appears).

Easily readable results can be obtained in the line-scan mode. Two mutually perpendicular directions have to be used, since the possible asymmetry has two independent parameters, namely the amplitude and the orientation.

Key words: Scanning analytical electron microscopy, Auger microprobe, energy analyzers, cylindrical mirror analyzer, ring shaped electron detector, microprobe adjustment.

Address for correspondence:

L. Frank

Institute of Scientific Instruments, Czechoslovak  
Academy of Sciences, Královopolská 147, 612 64 Brno,  
Czechoslovakia

Phone: 42 - 5 - 749292

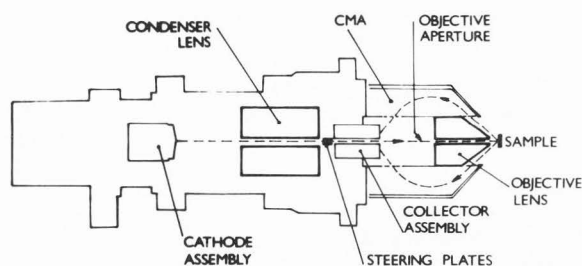


Fig. 1. : Simplified cross-section of the PHI 595 Multiprobe.

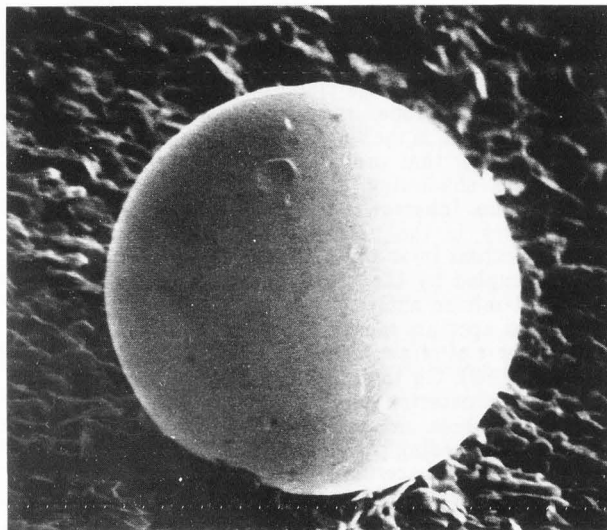


Fig. 2. : SEM image of the Cr sphere (78  $\mu\text{m}$  diameter) on the carbon paste.

The line-scans were taken horizontally and vertically (with respect to the field of view) across the cap of the sphere for Auger electrons of the main surface contaminants, i.e. for C KLL 265 eV and O KLL 509 eV peaks and for three different energies of the background, namely 40 eV, 400 eV and 2500 eV. In the last three cases, the 'background' energy which is called for in the line-scan mode, was defined to be 0 eV where a low noise signal is present only. The other parameters of the experiment were: primary energy 3 keV, primary current 0.5 nA, 160 points/line, 5 sec/point for the oxygen peak, 2.5 sec/point for the carbon peak and 0.5 sec/point for the background emission. The energy resolution control knob was in the position corresponding to 0.85% value.

The results shown in Figs.3 and 4 demonstrate quite clearly the pronounced asymmetry of the detection efficiency with a maximum somewhere in the bottom right quadrant of the field of view (scans are taken from left to right and from top to bottom). It may be noticed that

- the dependences can be considered as linear in the neighbourhood of the sphere cap,
- the slope of the linear part does not visibly depend on the energy for the background emission,
- but it is substantially different for each Auger scan.

The other interesting details of the curves, e.g. strong dependence of the marginal enhancement of the background signal (the edge effect - Shimizu et al., 1978 and Gerlach, 1985) on the energy and its comparison with the edge effect at the Auger scans, fall outside the scope of this paper and will be discussed elsewhere.

A straight line is fit to the scan curves in the neighbourhood of the centre of the spherical cap, so that the signal will be

$$I(r) = I(0) \left[ 1 + K \frac{r}{R} \right], \quad (1)$$

where  $R$  is the radius of the sphere and  $r \in (-R, R)$  the coordinate within the image of the sphere. Denoting the slopes extracted from the horizontal and the vertical scans as  $K_x$  and  $K_y$ , respectively, we obtain, from measurements shown in Figs.3, 4 and 10 (column  $K_x'$ , see later), the values given in Table 1.

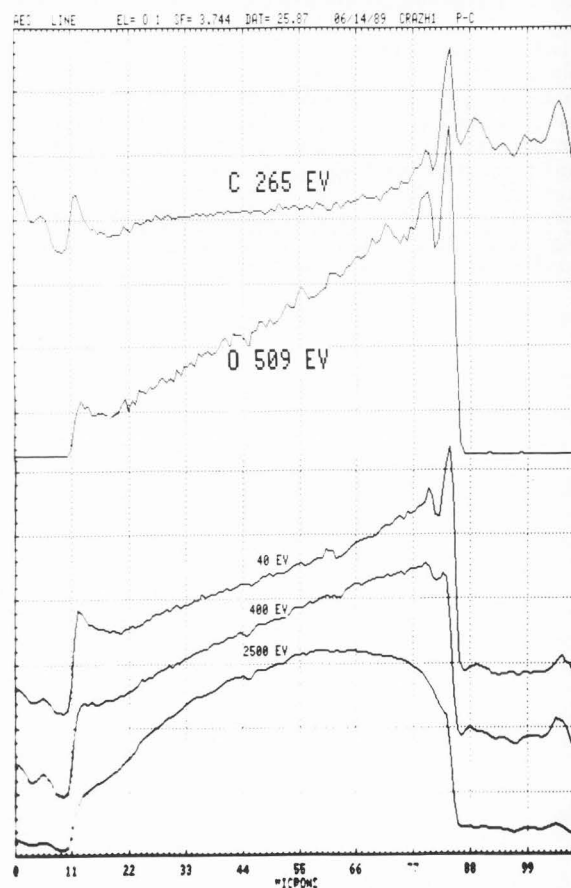


Fig. 3. : Set of line-scans (Auger peaks and energy of the background emission indicated) taken horizontally across the sphere of Fig. 2 (0.85% energy resolution).

The resulting values correspond, for example, to an increase in the background signal in the ratio 1:2.6 across the whole sphere in the x direction. Such a result is unexpected and unfavourable for instrument operation.

Sensitivity variations in the Auger microprobe

Table 1 : The slopes of the measured line-scans

scan	$K_x$	$K_y$	$K_x^{-1}$
O KLL 509 eV	0.95	0.088	0.49
C KLL 265 eV	0.21	0.35	0.19
SE 40 eV	0.44	0.21	0.21
SE 400 eV	0.46	0.21	0.21
SE 2500 eV	0.47	0.23	0.20

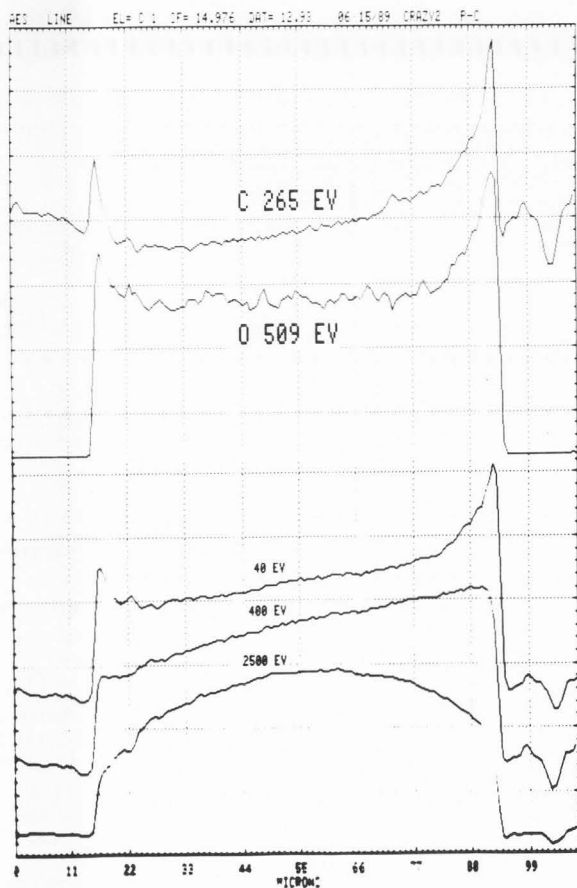


Fig. 4. : The same line-scans as in Fig. 3, vertical direction.

Model

In order to model the situation it is first necessary to make some reasonable assumptions about the angular distribution of the electron emission. It has been reported (Seah and Hunt, 1988) that:

- a) up to an emission angle of  $70^\circ$  from the surface normal the cosine distribution is valid for both the Auger and the background emission,
- b) up to an angle of incidence of about  $30^\circ$  the peak-to-background ratio is constant.

Combining (a) and (b), we can state that at least within the neighbourhood of the cap we can consider both the Auger and the background electrons as having cosine distributions, so that

$$I(\theta_0) = I_0 \cos \theta_0 \, d\Omega \quad (2)$$

The angle between the general ray  $\vec{a}_1 = (\cos \varphi \sin \theta, \sin \varphi \sin \theta, \cos \theta)$  and the surface normal  $\vec{a}_2 = (\sin \alpha, 0, \cos \alpha)$  (where  $\sin \alpha = r/R$ , see Fig.5) is given as

$$\cos \theta_0 = \vec{a}_1 \cdot \vec{a}_2 = \sin \alpha \cos \varphi \sin \theta + \cos \alpha \cos \theta \quad (3)$$

and the measured signal is

$$I(r) = I_0 \int_0^{2\pi} \int_{\theta_A}^{\theta_A + \delta\theta} \left[ \frac{r}{R} \cos \varphi \sin \theta + \sqrt{1 - \frac{r^2}{R^2} \cos^2 \theta} \right] \sin \theta \, d\theta \, d\varphi \quad (4)$$

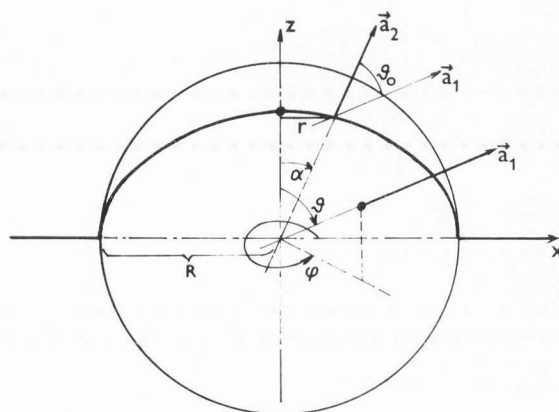


Fig. 5. : Definition of the angular coordinates.

The quantity  $\delta\theta$  represents the angular width of the detector which is now assumed to be  $\varphi$  dependent.

To determine this dependency we use the spherical trigonometry approach according to Fig.6. Given two sides,  $\eta$  and  $\theta_A + \Delta\theta$ , of the spherical triangle and the angle  $\varphi - \varphi_0$  opposite to the larger side ( $\theta_A + \Delta\theta > \eta$ ).  $\theta_A = 42.3^\circ$  is the mean analyzer entrance angle.  $\eta$  is the cone inclination representing the asymmetry due to misalignment and  $\Delta\theta$  is the nominal width of the hollow analyzed beam. Under these conditions we can use the standard formulae (Bartsch, 1979) to calculate the remaining side of the triangle,

$$\begin{aligned} \text{tg } \frac{\theta_{\max}}{2} &= \\ &= \text{tg } \frac{\theta_A + \Delta\theta + \eta}{2} \cos \frac{\varphi - \varphi_0 + \gamma}{2} \cos^{-1} \frac{\varphi - \varphi_0 - \gamma}{2} \quad (5) \end{aligned}$$

$$\sin \gamma = \sin \eta \sin(\varphi - \varphi_0) \sin^{-1}(\theta_A + \Delta\theta) \quad (6)$$

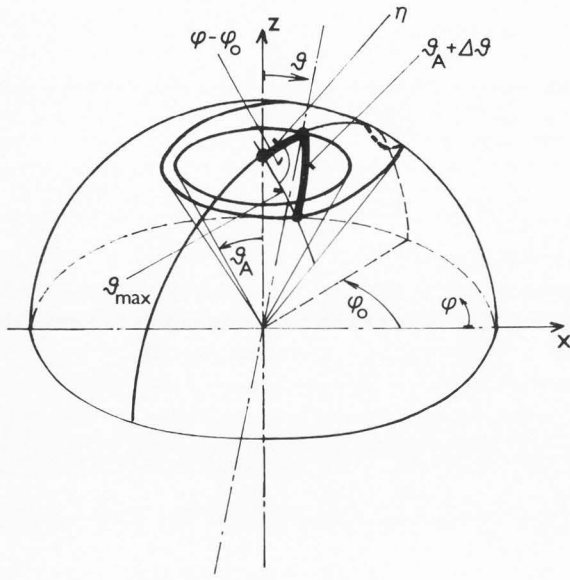


Fig. 6. : Geometry of the solid angular range of the analyzer acceptance limited by two mutually inclined cones;  $\theta_{max} = \theta_A + \delta\theta$ .

Noting that  $\eta \ll \theta_A$ ,  $\Delta\theta \ll \theta_A$  we can write

$$\gamma \approx \eta \frac{\sin(\varphi - \varphi_0)}{\sin \theta_A} \quad (7)$$

$$\frac{\cos \frac{\varphi - \varphi_0 + \gamma}{2}}{\cos \frac{\varphi - \varphi_0 - \gamma}{2}} \approx 1 - 2 \operatorname{tg} \frac{\varphi - \varphi_0}{2} \sin \frac{\gamma}{2} \approx$$

$$\approx 1 - \frac{2\eta}{\sin \theta_A} \sin^2 \frac{\varphi - \varphi_0}{2} \quad (8)$$

and

$$\operatorname{tg} \frac{\theta_A + \Delta\theta + \eta}{2} \approx \operatorname{tg} \frac{\theta_A}{2} \left[ 1 + \frac{\Delta\theta + \eta}{2s \sin \theta_A} \right], \quad (9)$$

$$\operatorname{tg} \frac{\theta_{max}}{2} \approx \operatorname{tg} \frac{\theta_A}{2} \left[ 1 + \frac{\delta\theta}{\sin \theta_A} \right]$$

Combining now eqs. (7) to (9) we obtain

$$\delta\theta \approx \Delta\theta + \eta \cos(\varphi - \varphi_0) \quad (10)$$

Our task is to estimate the slope of  $I(r)$  in the neighbourhood of  $r=0$ . From (4) we have

$$\left. \frac{dI}{dr} \right|_{r=0} = \frac{I_0}{R} \int_0^{2\pi} \int_{\theta_A}^{\theta_A + \delta\theta} \cos \varphi \sin^2 \theta d\theta d\varphi \approx$$

$$\approx \frac{I_0}{R} \sin^2 \theta_A \int_0^{2\pi} \delta\theta(\varphi) \cos \varphi d\varphi =$$

$$= \eta \frac{I_0}{R} \sin^2 \theta_A \int_0^{2\pi} \cos \varphi \cos(\varphi - \varphi_0) d\varphi =$$

$$= \pi \eta \frac{I_0}{R} \cos \varphi_0 \sin^2 \theta_A \quad (11)$$

The unknown scale factor  $I_0$  can be best determined from the signal value in the sphere centre:

$$I(0) = I_0 \int_0^{2\pi} \int_{\theta_A}^{\theta_A + \delta\theta} \cos \theta \sin \theta d\theta d\varphi \approx$$

$$\approx I_0 \sin \theta_A \cos \theta_A \int_0^{2\pi} \delta\theta(\varphi) d\varphi =$$

$$= 2\pi \Delta\theta I_0 \sin \theta_A \cos \theta_A \quad (12)$$

Dividing now eqs. (11) and (12) we get

$$\left. \frac{R}{I(0)} \frac{dI}{dr} \right|_{r=0} = K = \frac{\eta}{2\Delta\theta} \operatorname{tg} \theta_A \cos \varphi_0 \quad (13)$$

As  $K_y$  corresponds to the  $-y$  direction, the experimentally determined parameters are (see Fig.7):

$$K_x = \frac{\eta}{2\Delta\theta} \operatorname{tg} \theta_A \cos \varphi_0, \quad (14)$$

$$K_y = -\frac{\eta}{2\Delta\theta} \operatorname{tg} \theta_A \sin \varphi_0$$

and the parameters of the asymmetry are

$$\frac{\eta}{\Delta\theta} = 2 \operatorname{cotg} \theta_A (K_x^2 + K_y^2)^{1/2}, \quad (15)$$

$$\varphi_0 = \operatorname{arctg} \left[ -\frac{K_y}{K_x} \right]$$

Finally we substitute the values of  $K_x$ ,  $K_y$  from Table 1; the results are given in Table 2.

Table 2 : Final parameters of the asymmetry

scan	$\eta/\Delta\theta$	$\varphi_0$
O KLL 509 eV	2.10	-5.3°
C KLL 265 eV	0.90	-59.0°
SE 40 eV	1.07	-25.5°
SE 400 eV	1.11	-24.3°
SE 2500 eV	1.15	-26.1°

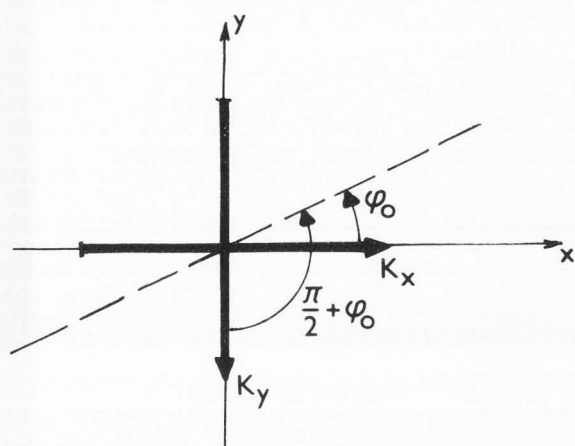


Fig. 7. : Decomposition of the asymmetry 'vector' into mutually perpendicular line-scans.

#### Discussion

- Examining the results in Table 2 we can see that:
- the non-realistic  $\eta/\Delta\theta$  values (slightly above 1) can be caused by the approximations used, the value 2.10 indicates deviations from the outgoing assumptions (i.e. the cosine distribution),
- deviations from coaxiality are quite large,
- neither parameter depends significantly on the energy of the background emission (in agreement with the behaviour of the measured curves),
- the parameters corresponding to the Auger line-scans differ not only in  $\eta/\Delta\theta$  but also in the angle  $\varphi_0$ .

The last point cannot be explained by the energy dependent rotation of the electron trajectory plane due to stray magnetic fields, because the effect does not occur when the background energy is changed. The only remaining possible explanation seems to be the large anisotropy of Auger emission causing the emission maximum to deviate at least  $20^\circ$  to  $30^\circ$  from the surface normal.

The remaining two points represent acceptable results of the study sufficient for explaining the observed phenomena.

Nevertheless, one needs to examine an alternative explanation of the whole effect as a result of a misalignment of the system, i.e. some deviations from coaxiality of the illuminating system and the analyzer.

The alignment is controlled by steering plates placed between the condenser and objective lens. Correct alignment is indicated by a stationary scanning electron microscope (SEM) image when the objective lens excitation is wobbled. The alignment was carried out for a primary energy of 3 keV and the slope  $K$  was immediately measured. Altering the excitation of the steering plates by 35% and 25%, respectively, which leads to a significant shift of the image, movements during wobbling and a three-fold decrease of the signal, the  $K$  value changes by 7% only.

Another means to visualize the alignment is to use a very low primary energy at minimum magnification. Then the image of the objective aperture appears on the screen and can be shifted by the steering plates. Fig. 8 shows the aperture in the SEM mode - the deviation

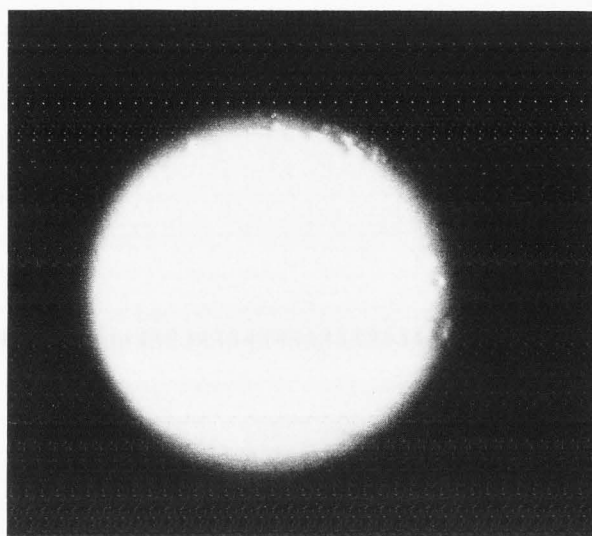


Fig. 8. : The objective aperture hole visible in 300 eV secondary electron image.

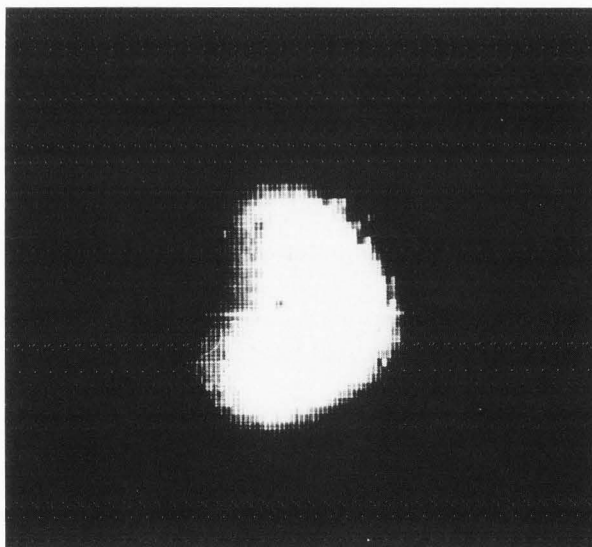


Fig. 9. : The aperture as projected onto a mapping taken at 300 eV (elastic peak).

from the centre of the field of view corresponds to a change in plate excitation amounting to 6% only. The back-scattered electron (BSE) image (Fig. 9) taken by means of the CMA at 300 eV exhibits the same deviation from the centre and, in addition, inhomogeneous illumination with the maximum oriented in exactly the same direction as proposed by Table 2. This can easily be explained by the mirror reflection of the electrons keeping the azimuthal angle with respect to the aperture centre.

As an additional piece of evidence, further line-scans were taken after changing the set-up of the energy resolution control. Fig. 10 corresponds to Fig. 3, except that the control knob was rotated one turn (down to an energy resolution of about 1.35%). The slopes  $K_x^1$  are listed in Table 1; the effect has obviously been reduced by roughly 50%. Such a change results (for  $\eta$  constant) in a 1.6-fold increase of  $\Delta\theta$  according to eq. (15), which is in exact agreement with the performed change in the resolution.

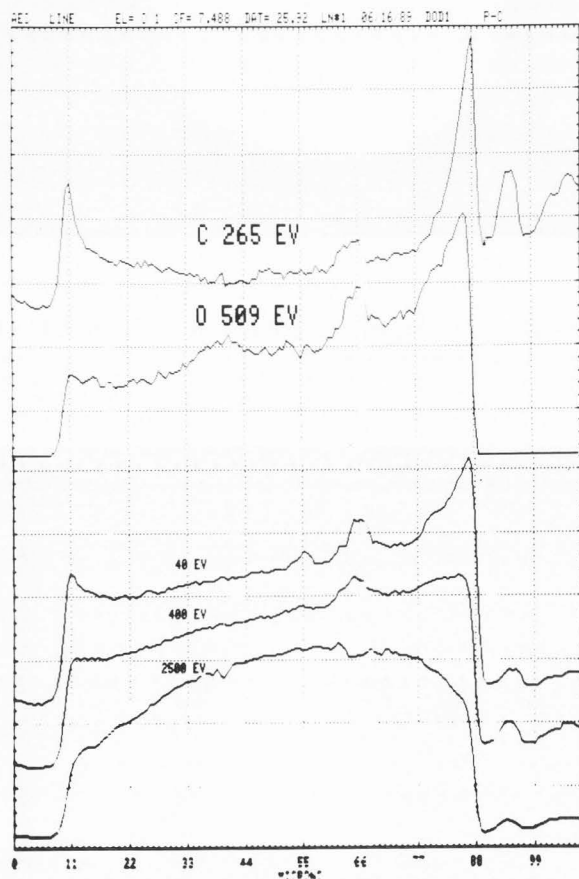


Fig. 10.: Set of horizontal line-scans across the Cr sphere for the energy resolution control adjusted to 1.35%.

Let us finally note that the channeltron in the Multiprobe used for the true detection has its axis at  $\varphi=0^\circ$ . Excessive electron extraction in the channeltron direction cannot be, therefore, responsible for the effect. As already mentioned, the angle  $\varphi_0$  does not depend on the energy of the background emission. This means that stray magnetic fields inside the CMA are negligible and the azimuthal angle of electron trajectories is conserved.

#### Conclusions

The data collected provides evidence that azimuthal variations of sensitivity take place in the examined device. As there is no reason to believe that the instru-

ment tested is not a typical example of instruments of this type, Multiprobe users are strongly recommended to test their systems in the way described. Precise work in the imaging modes evidently requires a much more reliable procedure for precentering the detector assembly or possibly the introduction of some method for centering the detector entrance aperture from outside.

Interesting are the differences in slopes of the Auger scans and between the slopes of the Auger and background scans. Although the technology of the sphere production is not exactly known, one can expect that the structure of the spheres is not very different from the single crystal character. The crystallinity of the sphere material probably induces the Auger emission anisotropy of the surface contaminants.

#### Acknowledgements

The experiments were carried out in the Institute of Physics, Technical University Clausthal. The author is indebted to Professor E. Bauer, Director of the Institute, for placing the Multiprobe laboratory at his disposal and for valuable and stimulating discussions of the problem.

#### References

- Bartsch HJ (1979) Taschenbuch mathematischer Formeln (Pocket-book of mathematical formulae). Fachbuchverlag, Leipzig, GDR, 394.
- Gerlach RL (1980) Optimization of the scanning Auger microprobe, in: Electron Microscopy 1980; III, P. Brederoo and V.E. Cosslett (eds.), EUREM foundation, Leiden, The Netherlands, 210–211.
- Gerlach RL (1985) The influence of sample and detector angles upon Auger electron signal, in: Electron optical systems for microscopy & microanalysis, SEM Inc., AMF O'Hare, Chicago, USA, 201–207.
- Seah MP, Hunt CP (1988) Auger electron spectroscopy: Method for the accurate measurement of signal and noise and a figure of merit for the performance of AES instrument sensitivity. Rev. Sci. Instrum. **59**, 217–227.
- Shimizu R, Everhart TE, MacDonald NC, Hovland CT (1978) Edge effect in high-resolution Auger-electron microscopy. Appl. Phys. Lett. **33**, 549–551.
- Risley JS (1972) Design parameters for the cylindrical mirror energy analyzer. Rev. Sci. Instrum. **43**, 95–103.

#### Discussion with Reviewers

**M.P. Seah:** It is clear that in any mechanical system the mispositioning or malfunction of components, either through wear and tear, or abuse, or through poor quality control in manufacture or through a design fault do occur and it is important to have simple and direct methods to diagnose them. It seems to me in this work that Figs. 3 and 10 go to the nub of the problem. If the problem arises solely through a variable resolution slit which is effectively narrower in one azimuth than another, two effects will occur:

- (i) As the slit is increased the intensities in all azimuths increase by the same amount but from different starting values. Thus, the differences between the intensities on the left and right in Fig. 10 should be the same as that in Fig. 3. The results do in fact agree very closely with this behaviour.
- (ii) If the low intensity to the left arises through the slit being narrower on that side, the energy resolution of the spectrum will be better. This is an easy experiment for

the author to do to confirm this hypothesis before publication.

**Author:** Having momentarily no possibility of carrying out new measurements I have selected two older spectra which were not taken exactly in points the azimuths of which with respect to the sphere centre are identical with directions towards the maximum and the minimum sensitivity but which still sufficiently demonstrate the effect (see Fig.11).

It cannot be recommended to replace the method proposed in the paper by the method of comparing peak widths in the spectra taken in several points lying on the sphere around its circumference and not far from its margin. There are two reasons for this: (i) For a specimen that has not been prepared 'in-situ' only contaminant peaks (of which the carbon peak is too broad to be suitable) can be utilized before ion beam cleaning, and (ii) by using the standard ion beam bombardment from the side, the spherical cap is not homogeneously cleaned so that peak width variations can be expected due to variations in chemical bonds.

**P. Kruit:** For an experimental evidence of asymmetric detection efficiency of the CMA it must be certain beyond doubt that the emission from the specimen is not asymmetric. This is not the case in the described experiment. Why not use a flat surface of non-crystalline material? Or alternatively: any kind of specimen which can be rotated such that asymmetric emission is averaged? Or at least: repeat the measurement on many different spheres.

**Author:** A flat surface cannot be used to demonstrate the effect because PHI 595 does not allow one to separate the emission according to the azimuthal angle (this is possible by shadowing by the sphere top only). Similarly, no sample rotation facilities are available in the device.

The measurement was repeated for many various spheres and qualitatively similar results were obtained. For example, the slopes  $K_x$  of 500 eV total emission scans across caps of seven various Pb spheres vary from 0.22 to 0.36 while  $K_y$  are within 0.10 to 0.27. These values give  $\eta/\Delta\theta \in (0.63, 0.89)$  and  $\varphi_0 \in (-20.3^\circ, -50.8^\circ)$ .

Such a dispersion of the asymmetry parameters can probably be ascribed to deviations from the supposed angular emission distribution due to specimen crystallinity. For practical application of the method, relatively large spheres of polycrystalline nature are recommended.

**P. Kruit:** Is it really impossible to mechanically change the alignment of the detector entrance aperture in order to show that its misalignment is indeed responsible for the asymmetry?

**Author:** The direct inspection and information from all available sources (including discussion with servicemen) prove that the device used does not allow this. Indirect control of the aperture position is possible through change of the aperture width only, as mentioned in the paper.

**P. Kruit:** Can you give a quantitative relation between the off-center distance of the aperture and the tilt angle of the acceptance cone?

**Author:** In the customer documentation the diameter of the ring shaped aperture is not mentioned so that the relative distances can be considered only with respect to the ring width as the length unit.

**P. Kruit:** How large is  $\Delta\theta$  in the circumstances of table 2 and why do you call the observed values of  $\eta/\Delta\theta$  non-realistic?

**Author:** The accepted angular spread  $\Delta\theta$  can be estimated from the FWHM energy resolution which was measured 0.85% for a point analysis. Suppose that the contributions to resolution resulting from the exit aperture size and from the angular spread are equal and that the base resolution is twice the FWHM resolution. Then we get the full angular width  $\Delta\theta \approx 13^\circ$  according to Risley (1972).

Equation (10) shows that the local angular beam width varies between  $\Delta\theta + \eta$  and  $\Delta\theta - \eta$  around the detector circumference. Therefore, only the values  $\eta \in (-\Delta\theta, \Delta\theta)$  can occur in practice, while  $\eta > \Delta\theta$  would also bring absurd negative contribution to the integral (11).

**P. Kruit:** How can we be sure that the asymmetry is not caused by

- (i) the specimen being off-center,
- (ii)  $\theta$ -dependent acceptance angle,
- (iii) detector asymmetry near the channeltron,
- (iv) charging of a contaminant or insulator.

**Author:** The reasons are following:

- (i) In the first approximation, an off-center position of the specimen (a sphere) would result in a shift of the energy window only so that the nonsymmetry of the line-scans would not appear for energy filtered background emission (SE curves) which slowly varies with energy.
- (ii) If I understand well, you inquire about possible deviations from the linear dependence of the actual sensitivity on the aperture width. These are not excluded in principle but both quantities are surely proportional which is sufficient for qualitative explanation of the effect.
- (iii) The maximum sensitivity does not fit to the azimuthal angle at which the channeltron is positioned.
- (iv) The effect is absolutely stable in time, independent of the primary energy and occurs repeatedly also in clean parts of metal spheres cleaned using ion beam bombardment.

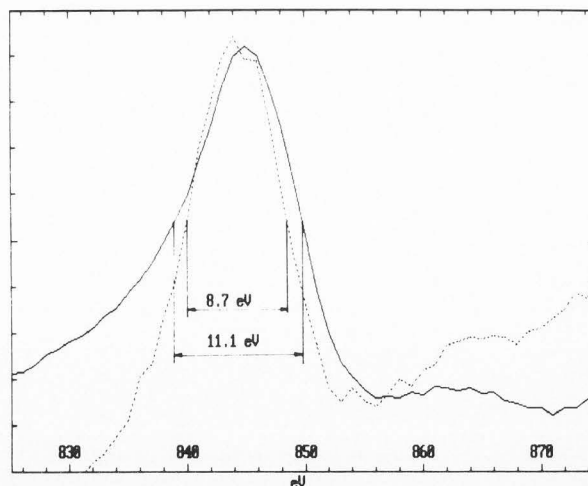


**Fig. 11.:** Ni 844 eV peak measured in two points on surface of Ni+Cr sphere; both spectra are scaled and offset to get identical net heights of the peaks. Points of analysis lie near the sphere margin, approx.  $60^\circ$  from the azimuth corresponding to the maximum sensitivity (full line) and again  $60^\circ$  from the azimuth of the minimum sensitivity (dashed line).

**G.E. McGuire:** The method of preparing the Cr should be expanded. In the 'Conclusion' the author suggest that this may be crystalline. In many studies it has been shown that the crystal orientation will influence the amount of C and O absorption on the surface.

**Author:** As mentioned in the paper, Cr spheres were extracted from metal powder available commercially as brazing filler for vacuum brazing (Nicrobraz 50, Wall Colmonoy Ltd., Pontardawe—Glam, UK); demonstration of the effect on widely available specimen appeared to be important. Details regarding the powder preparation are not known. Nevertheless, the influence of crystallinity can be judged on the basis of comparison of the results obtained for more spheres which, being simply attached with a paste onto a flat surface, are randomly oriented with respect to the instrument axis. See answer to the second question in the Discussion.

**R.L. Gerlach and R.R. Olson:** The 'Auger line scans' shown (and labeled as C or O) are the Auger peak height plus the background of inelastically scattered and secondary electrons at that energy  $[N(E_p)]$  (the 'background' energy was set to 0 eV as mentioned in 'Experimental'), rather than taking the 'Auger signal' as the peak height above background at each spatial point in the line scan. (The background  $[N(E_b)]$  is usually taken on the high kinetic energy side of the Auger peak, or an interpolated value of the background from measurements on both sides of the Auger peak.) What is the effect of the observed anisotropy on  $[N(E_p)-N(E_b)]$  line scans?

**Author:** This is a misunderstanding; the Auger line scans labeled as C or O are really  $[N(E_p)-N(E_b)]$  scans. The 'background' was set to 0 eV only when measuring the total emission scans (energy filtered background) which are labeled with energy values in figures and in Table 1 are indicated as SE curves.

**R.L. Gerlach and R.R. Olson:** Normalization procedures are typically used on SAM image data to suppress the influence of topography on the Auger image; these normalization procedures may also reduce the effect of anisotropy in the imaging system on the Auger images. These have not been considered by the author. What is the best normalization scheme to ameliorate the effects of the observed anisotropy in extracting the 'chemical image' from the measured Auger data?  $[N(E_p)-N(E_b)]/N(E_b)$  or  $[N(E_p)-N(E_b)]/[N(E_p)+N(E_b)]$  (see Prutton et al., 1981)?

**Author:** Both the Auger line scans shown in Fig.3 have been processed using both mentioned algorithms; the results are shown in Fig.12.

One can conclude from these curves that

- (i) differences between both algorithms are negligible, at least as far as the image of the sphere itself is concerned, and
- (ii) correction is unsuccessful. Inclination of the oxygen line-scan is not fully compensated and the carbon line-scan is overcompensated. Nevertheless, this is obvious from Fig.3: slopes of the background scans lie in between the slopes of both Auger line-scans.

**R.L. Gerlach and R.R. Olson:** What are the limitations of such normalization techniques? (i.e., for severely anisotropic systems where the terms in the denominators become very small?)

**Author:** Practical limitations may arise from excessive

degradation of the signal-to-noise ratio (SNR) in the normalized data. This is a topic for a separate study, so that only several notices will be presented here. Standard deviations of the normalized data were published (ElGomati et al., 1987). I propose to measure SNR by using the variation factor, i.e. the ratio of the standard deviation to the mean value. I am preparing a report about the study of SNR obtained in the normalizing techniques. From preliminary results of this study the following can be mentioned: If  $V[N(E)]$  is used for the variation factor of  $N(E)$  and  $x=[N(E_p)-N(E_b)]/N(E_b)=P/B$  (peak-to-background ratio), then

$$\begin{aligned} \{V[N(E_b)]\}^{-1} V\{[N(E_p)-N(E_b)]\} &= x^{-1}\sqrt{2+x} \\ \{V[N(E_b)]\}^{-1} V\{[N(E_p)-N(E_b)]/N(E_b)\} &= \\ &= x^{-1}\sqrt{(2+x)(1+x)} [1+(1+x)/P]^{-1} \\ &\quad \{V[N(E_b)]\}^{-1} x \\ &\quad \times V\{[N(E_p)-N(E_b)]/[N(E_p)+N(E_b)]\} = \\ &= 2x^{-1}(2+x)^{-1}\sqrt{2+3x+5x^2+2x^3} \end{aligned}$$

For Auger electron spectra, the relation  $x \ll 1$  is usually valid so that SNR is approximately the same in all cases approaching  $[\sqrt{2}/x]$ th multiple of the original SNR of the background. Because of the factor  $[1+(1+x)/P]^{-1}$ , the result of normalization with respect to  $N(E_b)$  can be slightly better for extremely low counts.

One can conclude that the mentioned normalization schemes do not significantly decrease the SNR of the net Auger signal  $N(E_p)-N(E_b)$  and their use is therefore not limited.

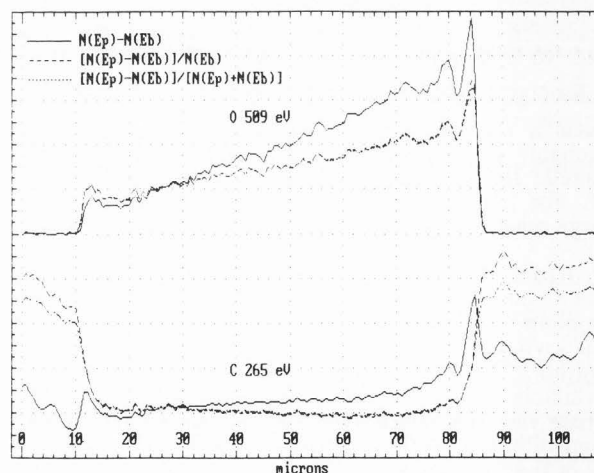


**Fig. 12:** The results of processing the Auger line scans shown in Fig.3 by normalization schemes that are most frequently applied to suppressing the topographical contrast.

**R.L. Gerlach and R.R. Olson:** Would the effects of the observed anisotropy be reduced by the use of multivariate imaging techniques (see ElGomati et al., 1987)?

**Author:** This technique transforms two Auger images into one scatter diagram so that two pixels having the same coordinates in both Auger images showing distributions of signals  $S_1 = N(E_{p1}) - N(E_{b1})$  and  $S_2 = N(E_{p2}) - N(E_{b2})$  correspond to point  $(S_1, S_2)$ . Points lying within the intersection of C and O line-scans with the sphere will obviously transform into some line indicating a correlation but no clusters of points revealing presence of chemically homogeneous regions will appear. I am not sure about the conclusions based on this fact.

**P. Kruit:** The aim of the paper is not quite clear: is it to warn PHI users, is it to suggest a solution to a general problem in CMAs?

**Author:** The aim was to suggest and to discuss a method suitable for testing the axial symmetry of the detection in PHI 595 Multiprobe or similar older systems and to recommend its application to PHI users.

**R.L. Gerlach and R.R. Olson:** It should be noted that the design of the analyzer which is the subject of this paper was modified in the manner suggested (external adjustments for centering of the detector assembly) in 1982 (Model 600 system).

**Author:** The paper is, of course, addressed mainly to users of the older instruments but it can be useful also for users of the adjustable system. It offers a method to check a proper adjustment.

#### Additional References

ElGomati MM, Peacock DC, Prutton M, Walker CG (1987) Scatter diagrams in energy analysed digital imaging: application to scanning Auger microscopy. *J. Microscopy* **147**, 149-158.

Prutton M, Peacock DC, ElGomati MM, Larson LA, Poppa H (1981) Normalisation of Auger electron images for beam current fluctuations and sample topography. in EMAG 81, Inst. Phys. Conf. Ser. **61**, 443-445.

